Salicylaldoxime-Supported Nona- and Tetrametallic Fe-III Cages

Salicylaldoxime-Supported Nona- and Tetrametallic Fe^{III} Cages

Kevin Mason[1], Alessandro Prescimone[1], Magnus Schau-Magnussen[2], Stergios Piligkos[2], Peter A. Tasker[1,*] and Euan K. Brechin[1,*]

[1]*EaStCHEM School of Chemistry, The University of Edinburgh, The Kings Buildings, West Mains Road, Edinburgh, EH9 3JJ, UK*

[2]*Department of Chemistry, University of Copenhagen, Universitetsparken 5, DK-2100, Denmark*

Abstract: The syntheses, structures and magnetic properties of seven new iron complexes, $[Fe_4O_2(sao)_4(tacn)_2]\cdot 2MeOH\cdot H_2O$ (**1**·2MeOH·H_2O), $[Fe_4O_2(Me\text{-}sao)_4(tacn)_2]\cdot 2MeCN$ (**2**·2MeCN), $[Fe_4O_2(Et\text{-}sao)_4(tacn)_2]\cdot MeOH$ (**3**·MeOH), $[Fe_9NaO_4(Et\text{-}sao)_6(hmp)_8]\cdot 3MeCN\cdot Et_2O$ (**4**·3MeCN·Et_2O), $[Fe_4(Et\text{-}sao)_4(hmp)_4]\cdot Et\text{-}saoH_2$ (**5**·Et-$saoH_2$), $[Fe_4(Ph\text{-}sao)_4(hmp)_4]\cdot 2MeCN$ (**6**·2MeCN) $[Fe_9O_3(sao)(pdm)_6(N_3)_7(H_2O)]$ (**7**), stabilised with salicylaldoxime ($saoH_2$) or derivatised salicylaldoxime (R-$saoH_2$) ligands in conjunction with either 1,4,7-triazocyclononane (tacn), 2-(hydroxymethyl)pyridine (hmpH) or 2,6-pyridinedimethanol ($pdmH_2$) are discussed.

Keywords: Fe^{III} coordination compounds, salicylaldoxime ligands, X-ray crystallography, SQUID magnetometry.

INTRODUCTION

Polynuclear clusters of iron are currently being studied for a variety of reasons [1, 2]. For example, bioinorganic chemists are synthesising cages in the hope of further understanding the role they play in the iron containing protein Ferritin that stores and regulates Fe within living organisms and can contain up to approximately 4500 metal centres [3-5]. The relatively large spin of the Fe^{III} ion also provides the possibility of these cluster molecules possessing large spin ground states and/or interesting magnetic properties [6]. The predominantly antiferromagnetic exchange between neighbouring Fe^{III} ions can result in geometric frustration, which can result in spin glass behaviour or the appearance of unusual jumps or plateaus in field dependent magnetisation measurements [6, 7]. Extended frustrated lattices such as the Kagome lattice [6] exhibit these phenomena, but they can also be witnessed on the molecular scale in antiferromagnetic $[Fe_3]$ triangles [7], $[Fe_{13}]$ Keggin ions [8] and $[Fe_{30}]$ icosidodecahedra [9, 10]. The ground states in such species are degenerate and/or have low lying excited states owing to the relatively low energy differences between different orientations of the spins [11]. These properties are also ideal for low-temperature magnetic refrigeration, with recent results demonstrating that molecules such as $[Fe_{14}]$ can outperform any conventionally employed solid state or intermetallic complexes by at least an order of magnitude [12].

Our work with Fe^{III} has been concerned principally with the pro-ligand salicylaldoxime ($saoH_2$, Fig. **1**) and its derivatives [13-17]. When mono-deprotonated, ($saoH^-$), the ligand forms a pseudomacrocyclic ring which has the perfect cavity size to accommodate a Cu^{II} ion [18-20]. This has led to extensive research within extractive hydrometallurgy as it is extremely selective over other metal ions, and is now responsible for extracting approximately 25% of the world's copper [21, 22]. Our interest also lies partly in its role as an anti-corrosive in protective coatings when treating lightly oxidised Fe surfaces, where it has been postulated that the protection occurs *via* polynuclear cluster formation on the surface [23]. A greater understanding of such clusters would therefore result in a more thorough understanding of the modes-of-action of the corrosion inhibition ability of the ligand [23].

To date we have explored the effects of systematically altering the reaction conditions within the rather simple Fe^{III}/R-$saoH_2$ reaction scheme, and have garnered a plethora of cages ranging in nuclearity from two to eight [13-17, 23-29]. Common to all the metallic skeletons are the triangular $[Fe_3O]^{7+}$ and tetrahedral $[Fe_4O]^{10+}$ building blocks. In the present work we employ co-ligands such as tacn, hmpH and $pdmH_2$ (Fig. **1**) in an attempt to introduce molecules that can compete with the phenolic oximes for the metal coordination sites and in the hope that novel coordination cages would form. The co-ligands were chosen based on their previous success in synthesising Fe^{III} clusters, as reported in the literature [30-39]. For example, the ligand tacn was used in the synthesis of the first recognised Fe^{III} Single-Molecule Magnet (SMM), $[Fe_8]$ [40, 41], and hmpH and $pdmH_2$ have both been used extensively in metal cluster synthesis [30-32, 35, 36, 42-51].

EXPERIMENTAL SECTION

Syntheses

All manipulations were performed under aerobic conditions using chemicals as received, unless otherwise stated. 2-hydroxyacetophenone oxime (Me-$saoH_2$) and 2-

*Address correspondence to this author at the EaStCHEM School of Chemistry, The University of Edinburgh, The Kings Buildings, West Mains Road, Edinburgh, EH9 3JJ, UK; Tel: +44 (0)131-650-7545;
E-mails: ebrechin@staffmail.ed.ac.uk, Peter.Tasker@ed.ac.uk

1877-945X/13 $58.00+.00

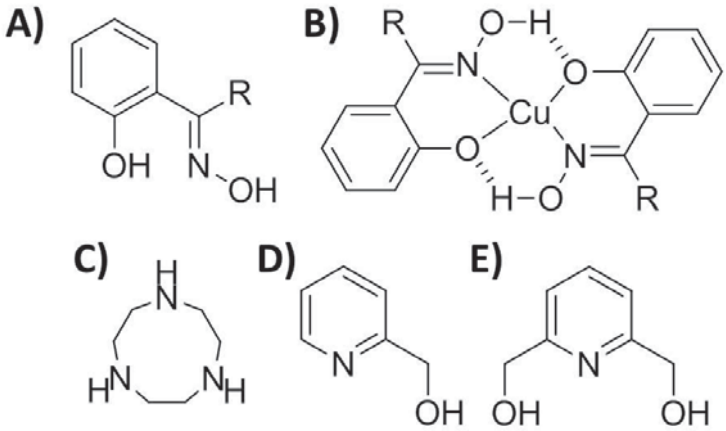

Fig. (1). (a) The ligands salicylaldoxime, R = H, $saoH_2$; R = Me, Me-$saoH_2$; R = Et, Et-$saoH_2$; R= Ph, Ph-$saoH_2$. (b) The pseudo-macrocyclic structure formed by mono-deprotonated salicylaldoxime copper extractants. (c) 1,4,7-triazacyclononane, tacn. (d) 2-(hydroxymethyl)pyridine, hmpH. (e) pyridine-2,6-dimethanol, $pdmH_2$.

hydroxypropiophenone oxime (Et-$saoH_2$) were synthesised *via* the reaction of the appropriate ketone with hydroxylamine and sodium acetate as described in the literature [52]. tacn was prepared as previously described [53].

$[Fe_4O_2(sao)_4(tacn)_2]\cdot 2MeOH\cdot H_2O$ (1·2MeOH·H_2O)

$FeCl_2\cdot 4H_2O$ (198 mg, 1 mmol) and $saoH_2$ (205 mg, 1.5 mmol) were stirred in a 1:1 mixture of MeOH and CH_2Cl_2 (25ml). In a separate flask tacn·3HBr (279 mg, 0.75 mmol) and NEt_3 (6ml, 54 mmol) were stirred in 5 ml of a 1:1 MeOH/CH_2Cl_2 mix. After 30 minutes the two independent solutions were added together and stirred for a further 18 hours, after which time the solution was filtered and left to evaporate slowly. X-ray quality crystals were present after 2 days in ~40% yield. Elemental analysis: found (calc. %) for $C_{40}H_{50}Fe_4N_{10}O_{10}$: C 45.23 (45.57), H 4.67 (4.78), N 13.21 (13.29).

$[Fe_4O_2(Me\text{-}sao)_4(tacn)_2]\cdot 2MeCN$ (2·2MeCN)

Procedure as for **1**, replacing $saoH_2$ with Me-$saoH_2$ (226 mg, 1.5 mmol) and MeOH with MeCN. Yield ~40%. Elemental analysis found (calc %) for $C_{44}H_{58}Fe_4N_{10}O_{10}$: C 47.46 (47.59), H 5.03 (5.26), N 12.25 (12.61).

$[Fe_4O_2(Et\text{-}sao)_4(tacn)_2]\cdot MeOH$ (3·MeOH)

Procedure as for **1**, replacing $saoH_2$ with Et-$saoH_2$ (165 mg, 1 mmol). X-ray quality crystals were grown by Et_2O diffusion into the MeOH solution in ~40% yield after 1 week. Elemental analysis: found (calc %) for $C_{48}H_{66}Fe_4N_{10}O_{10}$: C 49.11 (49.42), H 5.52 (5.70), N 11.47 (12.01).

$[Fe_9NaO_4(Et\text{-}sao)_6(hmp)_8]\cdot 3MeCN\cdot Et_2O$ (4·3MeCN·Et_2O)

$FeCl_2\cdot 4H_2O$ (298 mg, 1.5 mmol), Et-$saoH_2$ (165 mg, 1 mmol), hmpH (163 mg, 1.5 mmol) and NaOMe (135 mg, 2.5 mmol) were stirred in MeCN for 18 hours. The solution was filtered and then diffused with Et_2O. X-ray quality crystals grew during 5 days in approximately 30% yield. Elemental analysis: found (calc %) for $C_{99.50}H_{102}Fe_9N_{13}NaO_{25.20}$: C 49.21 (49.61), H 3.92 (4.27), N 7.25 (7.56).

$[Fe_4(Et\text{-}sao)_4(hmp)_4]\cdot Et\text{-}saoH_2$ (5·Et-$saoH_2$)

$FeCl_2\cdot 4H_2O$ (298 mg, 1.5 mmol), Et-$saoH_2$ (165 mg, 1 mmol), hmpH (163 mg, 1.5 mmol) and $Ca(OMe)_2$ (255 mg, 2.5 mmol) were stirred in MeCN for 18 hours. After filtration the solution was left to evaporate slowly, producing X-ray quality crystals after 5 days. Yield ~25%. Elemental analysis: found (calc %) for $C_{69}H_{71}Fe_4N_9O_{14}$: C 56.16 (56.23), H 4.64 (4.86), N 8.31 (8.55).

$[Fe_4(Ph\text{-}sao)_4(hmp)_4]\cdot 6MeCN$ (6·6MeCN)

$FeCl_2\cdot 4H_2O$ (397 mg, 2 mmol), Ph-$saoH_2$ (416 mg, 2 mmol), hmpH (327 mg, 3 mmol) and NaOMe (162 mg, 3 mmol) were stirred in MeCN for 18 hours. The solution was filtered and left to evaporate slowly for 3 days, during which time X-ray quality crystals grew in ~25% yield. Elemental analysis: found (calc %) for $C_{80}H_{60}Fe_4N_8O_{12}$: C 62.43 (62.04), H 4.02 (3.90), N 7.40 (7.23).

$[Fe_9O_3(sao)(pdm)_6(N_3)_7(H_2O)]$ (7)

$Fe(BF_4)_2\cdot 6H_2O$ (337 mg, 1 mmol), $saoH_2$ (68 mg, 0.5 mmol), $pdmH_2$ (278 mg, 2 mmol) and NaN_3 (130 mg, 2 mmol) were stirred in a 1:1 mix of MeCN/MeOH (30ml). The solution was heated to 50˚C and stirred for a further 3 hours. After filtering off a brown precipitate, the solution was allowed to evaporate slowly. X-ray quality crystals grew during three days in ~20% yield. Elemental analysis: found (calc. %) for $C_{49}H_{49}Fe_9N_{28}O_{18}$: C 32.53 (32.32), H 3.09 (2.71), N 21.28 (21.54).

PHYSICAL MEASUREMENTS

Elemental analyses were performed by the EaStCHEM microanalysis service. Direct current magnetic susceptibility measurements were carried out on a Quantum Design MPMS-XL SQUID magnetometer equipped with a 7T magnet. Eicosane was used to restrain the microcrystalline samples and diamagnetic corrections were applied using Pascal's constants. Single crystal X-ray crystallography for complexes **1**, **2**, **6**, and **3**, **4**, **5**, **7** was performed using a Bruker Smart Apex II CCD diffractometer equipped with an Oxford

Table 1. Crystallographic Details for Complexes 1-7

	1·2MeOH·H_2O	**2·2MeCN**	**3·MeOH**	**4·3MeCN·Et_2O**	**5·Et-saoH_2**	**6·6MeCN**	**7**
M, gmol^{-1}	1136.40	1274.60	1197.25	2606.07	1473.75	1756.07	1820.73
crystal system	Triclinic	Monoclinic	Monoclinic	Triclinic	Triclinic	Tetragonal	Orthorhombic
space group	*P*-1	$P2_1/c$	$P2_1/c$	*P*-1	*P*-1	$I4_1/a$	$Pna2_1$
a, Å	11.7667(14)	12.4265(3)	15.0460(3)	16.3371(5)	12.4159(7)	18.619(4)	29.2462(9)
b, Å	11.9297(15)	14.7726(4)	16.9478(4)	17.1987(11)	16.4389(7)	18.619(4)	17.0864(6)
c , Å	17.708(2)	16.5738(5)	21.1677(5)	25.7824(9)	17.9303(9)	25.806(5)	14.8911(6)
α, deg	77.837(6)	90	90	88.455(4)	73.102(4)	90	90
β, deg	76.857(6)	106.032(3)	102.437(2)	71.706(3)	89.225(4)	90	90
γ, deg	76.716(6)	90	90	64.484(4)	68.303(5)	90	90
V , Å^3	2322.6(5)	2924.14(14)	5271.0(2)	6157.5(6)	3235.3(3)	8946(3)	7441.3(5)
T , K	100(2)	100(2)	100(2)	100(2)	150(2)	100(2)	100(2)
Z	2	2	2	2	2	4	4
$\rho_{, calc}$ [g cm^{-3}]	1.625	1.448	1.490	1.41	1.513	1.304	1.625
crystal shape and colour	black block	brown block	black block	black block	black block	black block	black block
crystal size [mm]	0.13 x 0.13 x 0.13	0.23 x 0.14 x 0.12	0.20 x 0.15 x 0.04	0.52 x 0.33 x 0.21	0.45 × 0.17 × 0.05	0.11 x 0.09 x 0.07	0.07 x 0.04 x 0.04
μ, [mm^{-1}]	1.300	1.040	9.207	8.876	7.669	0.702	14.339
unique data	9510	6595	10298	13409	8912	3913	9362
unique data, (I > 2σ(F))	7739	5212	5332	11558	7314	2906	7278
[a]$R1$, [b]wR_2	0.0578, 0.1592	0.0430, 0.0716	0.0740, 0.0648	0.0655, 0.0622	0.0359, 0.0797	0.0688, 0.0684	0.0953, 0.0982
goodness of fit	1.104	1.151	1.1218	1.2051	1.021	1.0533	1.1201

[a] $R1 = \Sigma||F_o|-|F_c|| / \Sigma(|F_o|$ observed reflections.

[b] $wR_2 = [\Sigma w(|F_o^2| - |F_c^2|)^2 / \Sigma w|F_o^2|^2]^{1/2}$ for all data

Cryosystems LT device, using Mo-Kα, and an Oxford Diffraction SuperNova Dual diffractometer equipped with an Oxford Cryosystems LT device using Cu-Kα radiation, respectively. Data collection parameters and structure solution and refinement details are listed in Table **1**. Full details can be found in the deposited CIF files, CCDC 928056 - 928062.

RESULTS AND DISCUSSION

Synthesis

The general synthetic strategy adopted in this work was the introduction of co-ligands into our previously successful reaction schemes that examined the coordination chemistry of R-saoH_2 ligands with $Fe^{II/III}$ salts, in order to understand the effect of these co-ligands on the structural identity of the resultant cluster compound [13-17, 23-29]. The reaction of $FeCl_2·4H_2O$, saoH_2 and tacn in MeOH/CH_2Cl_2 with an excess of NEt_3 affords the tetrametallic 'butterfly' complex **1**. It is interesting to note that the only previously reported Fe clusters stabilised purely by R-saoH_2 ligands are the tetrametallic cubes, $[Fe_4(Me\text{-}sao)_4(Me\text{-}saoH)_4]·MeOH$ and $[Fe_4(sao)_4(saoH)_4]·saoH_2·C_8H_{10}$ [13,23]. The same reaction, employing Me-saoH_2 and Et-saoH_2 instead of saoH_2 and with the CH_2Cl_2 replaced with MeCN affords the structurally analogous complexes **2** and **3**, respectively. It is therefore clear to see that the change in the phenolic oxime, the change of solvent and indeed any change to the ratio of reactants employed, has no effect on the identity of the product, suggesting that the rigid, triangular face-capping tacn ligand is the dominant structural player. This contrasts sharply to reactions performed in the absence of tacn, in which all these reaction variables do have prominent effects on the identity of the product [13-17, 23-29]. The reaction of $FeCl_2·4H_2O$, Et-saoH_2, hmpH and NaOMe in MeCN yields the large and unusual nonametallic complex **4**. The reaction can be considered *similar* to that which produced the butterfly complexes **1**-**3**, but in which the tacn has been replaced by hmpH. The molecule, **4**, therefore represents the difference between employing a rigid chelating ligand with one dominant coordination mode, versus a flexible ligand which can possess numerous coordination modes – both chelating and bridging. The presence of a single Na^+ ion at the centre of the cluster suggested that the identity of the alkali metal ion used in the base would also have an important structure-directing role. Unfortunately we failed to isolate crystalline

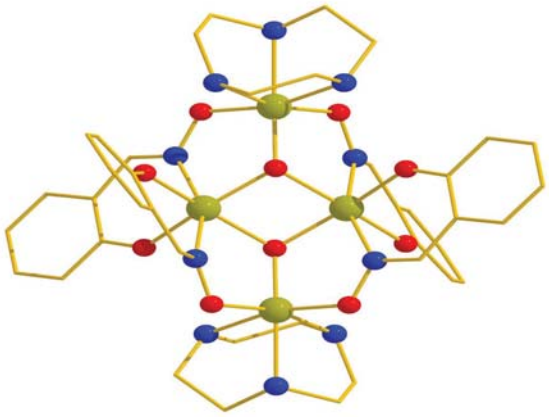

Fig. (2). The molecular structure of **1**. Colour code: Fe = olive green, O = red, N = blue, C = gold. H-atoms have been omitted and the molecule shown in ball and stick model neglecting thermal ellipsoids for clarity.

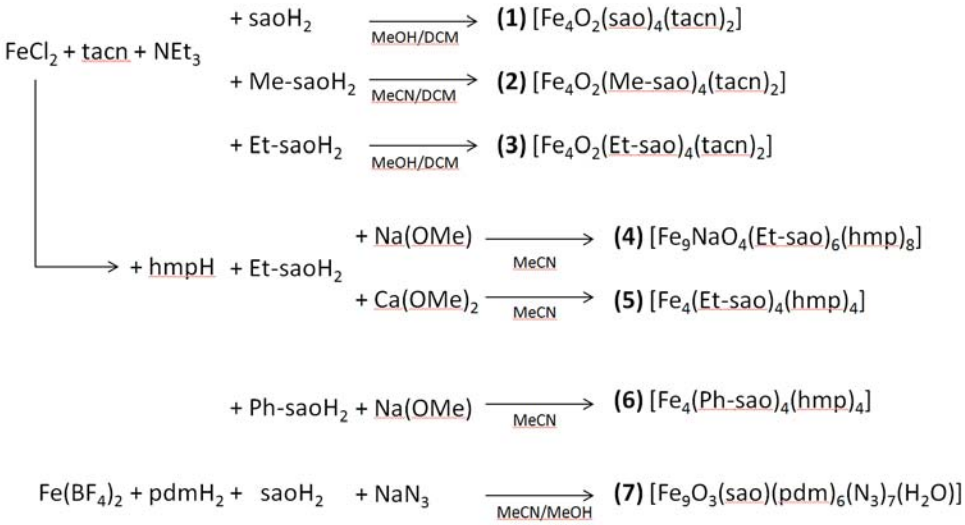

Scheme (1). A simplified schematic of the syntheses of complexes **1**-**7,** omitting co-crystallised species for clarity.

material from the use of other group 1 alkali metal cations (Li^+, K^+, Cs^+); however we were successful with $Ca(OMe)_2$, isolating the tetranuclear square complex **5** in which there is no Ca^{2+} present. Interestingly, although highly unusual, the [Fe^{III}_4] square topology is reminiscent of another oxime-based, F-bridged square we published recently (*vide infra*) [17]. Repetition of the reaction which produces complex **5**, but replacing Et-saoH$_2$ with other R-saoH$_2$ family members does not produce any crystalline material, but perhaps somewhat oddly, repetition of the reaction which produces complex **4**, but replacing Et-saoH$_2$ with Ph-saoH$_2$ does produce the [Fe^{III}_4] square, **6**. In this instance we presume that it is the steric bulk of the oximic Ph-group that is the dominant structural factor. Indeed a close inspection of nonametallic complex **4** suggests that the replacement of the Et-group with a Ph-group would likely be problematic from a simple steric consideration. This therefore gives us two routes to change from the large [Fe_9] complex to the smaller [Fe_4] complex: changing the charge on the cation, and/or increasing the bulk of the ketoxime group. Switching from the hmpH ligand to the closely related pdmH$_2$ produces a second nonametallic cage: the reaction of Fe(BF$_4$)$_2$·6H$_2$O, saoH$_2$, pdmH$_2$ and NaN$_3$ in MeOH/MeCN yields complex **7**. A direct comparison of the formulae of **4** and **7** suggests the pdm^{2-} ligand to be more dominant than the hmp^- ligand; the pdm^{2-}:R-sao^{2-} ratio being 6:1 and the hmp^-:R-sao^{2-} ratio being 1.33:1. All of these complexes were synthesised from ferrous salts and could not be reproduced with ferric salts.

Description Of Structures

The molecular structures of complexes **1**-**3** are analogous, differing only in the identity of the R-sao^{2-} ligand, and so for the sake of brevity we describe only complex **1**. Centrosymmetric complex **1** (Fig. **2**) crystallises in the triclinic space group *P*-1 with two (analogous) [Fe_4] molecules present in the unit cell. The metallic skeleton describes two edge-sharing [Fe^{III}_3] triangles or, perhaps more conventionally, a [Fe^{III}_4] 'butterfly'. Each triangle is scalene by strict definition, but isosceles based on ligand bridging modes. Central to each triangle is one μ_3-O^{2-} ion, forming the common [Fe^{III}_3O]$^{7+}$ moiety (or the [$Fe^{III}_4O_2$]$^{8+}$ butterfly), with the two unshared edges of the triangle bridged by sao^{2-} ligands in a familiar η^1:η^1:η^1:μ-mode. These lie alternately above and below the [Fe^{III}_4] plane. The two η^3-tacn ligands each chelate a 'wing-tip' Fe^{III} ion completing the [O_3N_3] donor set at this ion. These ions lie in distorted octahedral geometries that are

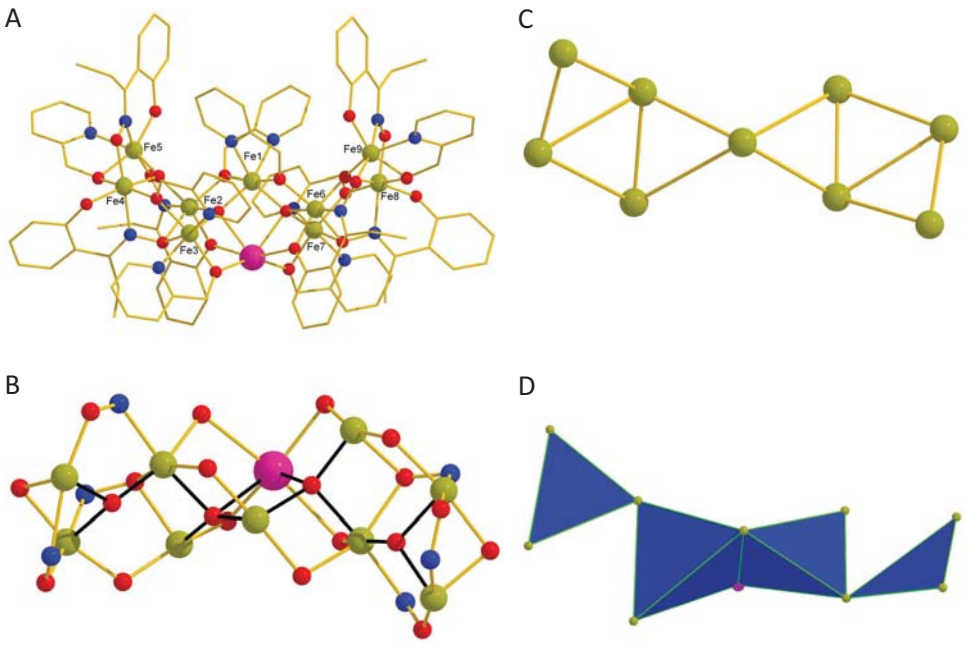

Fig. (3). **a**) The molecular structure of **4**. **b**) The core of **4**; the black bonds highlight the bonding modes of the oxide ions. **c**) The metallic skeleton of **4**. **d**) Triangular and tetrahedral building blocks based on the oxide ions. Colour code: Fe = olive green; O = red; N = blue; C = gold; Na = magenta. H-atoms have been removed for clarity.

perhaps best described as trigonal-antiprismatic; the face-capping tacn ligands forcing a trigonal distortion (Fe…N, ~2.2 Å; Fe…O, ~1.9 Å). The 'body' Fe^{III} ions have $[O_4N_2]$ donor sets and lie in distorted octahedral environments with the four 'equatorial' Fe…O distances measuring ~2.0 Å, and the two 'axial' Fe…N distances being ~2.2 Å.

There are four intra-molecular H-bonds between the monodentate phenolic O-atoms of the sao^{2-} ligands and the N-atoms of the tacn ligands (O…N, 2.850(5)-3.035(5) Å). The N-atoms and the oximic O-atoms are also involved in H-bonding to the H_2O and MeOH molecules in the lattice (2.754(4) – 3.062(7) Å). The closest cluster…cluster interactions occur between C-atoms in the phenolic oxime ligands at a distance of ~3.3 Å. Complex **2** is the Me-sao^{2-} analogue and complex **3** the Et-sao^{2-} analogue of **1**. There are no significant structural differences between the three complexes. Both **2** and **3** however crystallise in the monoclinic space group $P2_1/c$ and this affords differences in the manner that the molecules pack in the crystal. The closest literature precedent for **1**-**3** are the complexes $[Fe_4O_2(tacn)_2(sao)_2(O_2CR)_2]$ reported by Chaudhuri and co-workers in which carboxylates bridge wing-tip and body Fe ions [25, 26].

Complex **4** crystallises in the triclinic space group *P*-1 (Fig. **3**). The metallic skeleton (Fig. **3c**) comprises a series of edge- and vertex-sharing $[Fe^{III}_3]$ triangles. When also considering the four O^{2-} ions (2 x μ_4, 2 x μ_3) the core of the molecule can be described as two central $[Fe^{III}_3NaO]^{8+}$ tetrahedra sharing an edge, with both corners (at Fe6 and Fe2) connected to a peripheral $[Fe^{III}_3O]^{7+}$ triangle (Fig. **3d**). The triangular units contain the $[Fe^{III}_3O(sao)_3]^{+}$ building block, commonly observed in M^{III}/R-sao^{2-} coordination chemistry. Each triangle is linked to a tetrahedron through a $\eta^1{:}\eta^1{:}\eta^2{:}\mu_3$-Et-$sao^{2-}$ (Fe2-Fe3 and Fe6-Fe7) ligand and one $\eta^1{:}\eta^2{:}\mu$-hmp^- ligand (Fe3-Fe4 and Fe7-Fe8). The additional edges on each triangle (Fe8-Fe9 and Fe4-Fe5) are bridged *via* one $\eta^1{:}\eta^1{:}\eta^1{:}\mu$-Et-$sao^{2-}$ and one $\eta^1{:}\eta^2{:}\mu$-hmp^-. All remaining bridging within the central tetrahedra are *via* $\eta^1{:}\eta^1{:}\mu$-hmp^- ligands (Fe3-Na1, Fe1-Fe2, Fe1-Fe6 and Fe7-Na1). All the Fe^{III} ions lie in distorted octahedral geometries with *cis* angles in the range 73.54-114.17° and *trans* angles in the range 152.17-176.60°. There are two different coordination spheres present for the Fe^{III} ions: $[O_5N]$ for Fe4, Fe2, Fe6 and Fe8, and $[O_4N_2]$ for Fe5, Fe3, Fe1, Fe7 and Fe9. The Na^+ ion is six coordinate and in a very distorted environment, coordinated to six O-atoms, with bond lengths of ~2.3 Å to the two hmp^- O-atoms, ~2.4 Å to the two O^{2-} ions and ~2.6 Å to the phenolic O-atoms of the Et-sao^{2-} ligand. There are no intra- or inter-molecular H-bonds, with the shortest inter-molecular interactions occurring between phenolic O-atoms from the Et-sao^{2-} ligands and C-atoms on the pyridyl ring of the hmp^- ligands, at a distance of approximately 3.2 Å. Complex **4** is the largest nuclearity Fe^{III} cluster to be synthesised containing any R-$saoH_2$ ligand and joins a relatively small family of iron complexes of nuclearity nine: a search of the CCDC database (Version 5.33, Nov 2011) reveals only 73 Fe_9 molecules in comparison with the 535 characterised Fe_6 molecules, for example.

Complex **5** (Fig. **4**) crystallises in the triclinic space group *P*-1 with one Fe cluster and one Et-$saoH_2$ ligand in the asymmetric unit. The metallic core of **5** describes a distorted $[Fe^{III}_4]$ square with Fe…Fe lengths of 3.459(1)-3.474(1) Å and Fe-Fe-Fe angles of 86.97(2)-88.53(2)°. Each edge is bridged by a combination of one Et-sao^{2-} ligand bridging in a $\eta^1{:}\eta^1{:}\eta^1{:}\mu$-fashion and one hmp^- ligand bridging in a $\eta^1{:}\eta^2{:}\mu$-fashion. These lie alternately above and below the $[Fe^{III}_4]$ "plane". In fact the $[Fe_4]$ square is very distorted and non-planar as can be seen from Fig. (**4c**). Each iron ion is in the 3+ oxidation state and lies in an octahedral geometry with a $[O_4N_2]$ donor set, with *cis* angles of 75.55(1)-105.18(1)° and

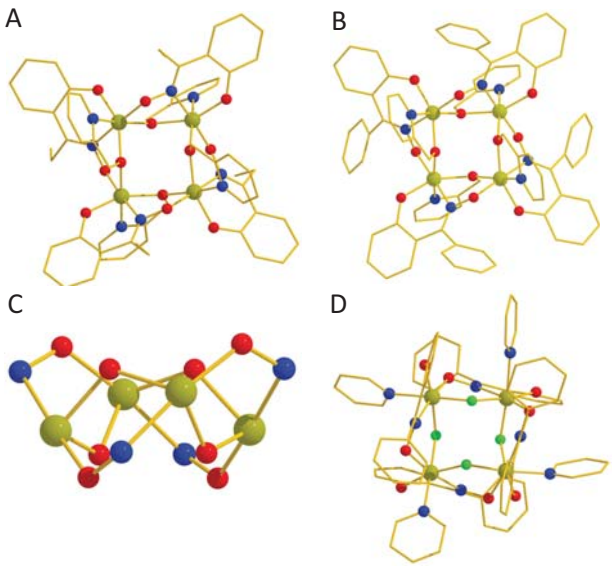

Fig. (4). The molecular structures of complexes (**a**) **5** and (**b**) **6** viewed perpendicular to the [Fe_4] face. (**c**) The structure of **6** viewed parallel to the [Fe_4] face highlighting the non-planar nature of the square. (**d**) The structure of the previously published complex [Fe_4F_4(Ph-sao)$_4$(py)$_4$].

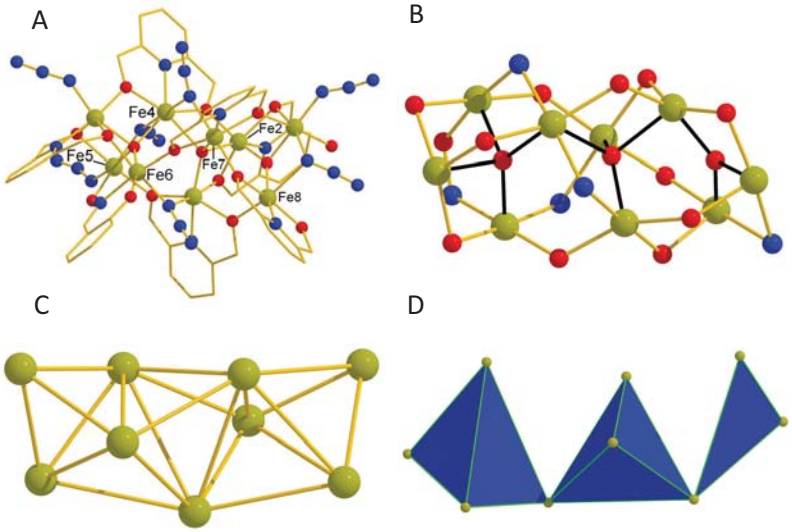

Fig. (5). **a**) The molecular structure of **7**. **b**) The core of the molecule with black bonds highlighting the coordination of the O^{2-} ions. **c**) The metallic skeleton of complex **7**. **d**) Triangular and tetrahedral building blocks based on oxide centres. Colour code: Fe = olive green; O = red; N = blue; C = gold. H-atoms have been removed for clarity.

trans angles of 152.32(1)-175.39(1)°. There is an inter-molecular H-bond to the co-crystallised Et-saoH$_2$ molecule in the lattice, between the phenolic O-atom of the coordinated oxime ligand and the oximic O-atom of the non-coordinated Et-saoH$_2$ molecule (O…O, 2.691(4) Å). The closest cluster…cluster interactions are of the order of 3.4 Å between C-atoms on neighbouring Et-sao^{2-} ligands. Complex **6** crystallises in the tetragonal space group $I4_1/a$ with one molecule in the asymmetric unit and four within the unit cell (Fig. **4**). The cluster is isostructural with complex **5**, differing only in the identity of the R-saoH$_2$ ligand. Symmetry now forces all of the Fe…Fe distances to be equivalent (3.451(1) Å) and the Fe-Fe-Fe angles are 86.33(2)˚ - again describing a distorted, non-planar [Fe_4] square. The octahedral Fe^{III} ions have *cis* angles in the range 80.25(1)-104.6(1)° and *trans* angles in the range 154.89(1)-173.52(1)°. There are a number of inter-molecular interactions within the crystal lattice, most notably π-π stacking between two neighbouring hmp$^-$ ligands (C…C, ~3.3 Å), with the shortest inter-molecular distance being between a phenolic O-atom and the pyridyl C-atoms of an hmp$^-$ ligand (O…C 3.208(6) Å). Clusters with the [Fe^{III}_4] square topology are very rare – indeed a search of the CCDC database returns only 8 hits when all bridges are the same (47 total). Interestingly however, complexes **5** and **6** are very similar to the complex [Fe_4F_4(Ph-sao)$_4$(py)$_4$] which we reported recently [15]. A comparison of the structures is given in Fig. (**4**). It is easy to see that the μ-F$^-$ and the terminally bonded pyridine in the latter complex have simply been replaced by the hmp$^-$ ligand in **5** and **6** which combines both coordination modes.

Complex **7** crystallises in the orthorhombic space group $Pna2_1$ (Fig. **5**). The metallic skeleton consists of six fused [Fe^{III}_4] tetrahedra with each tetrahedron sharing a face with

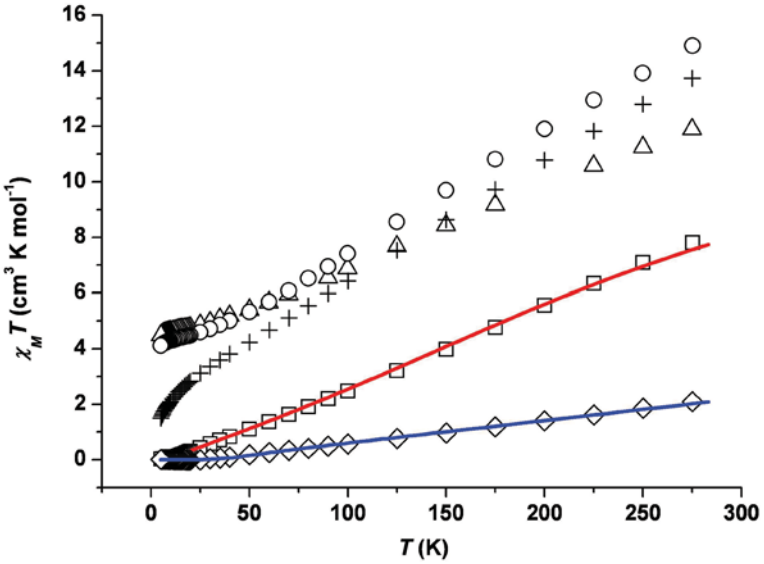

Fig. (6). Plot of $\chi_M T$ vs T for complexes **2** (◊), **4** (Δ), **6** (□) and **7** (○). The solid blue and red lines represent a fit of the experimental data of **2** and **6** respectively, as detailed in the text. A plot of the previously synthesised complex $[Fe_4F_4(Ph\text{-}sao)_4(py)_4]$ is shown for comparison (+).

its neighbour. Central to the molecule are three O^{2-} ions, two bonding in a μ_4-fashion and one bonding in a μ_3-fashion (Fig. **5b**). The core can thus be described as two $[Fe^{III}{}_4O]^{10+}$ tetrahedra sharing a vertex (at Fe4) with an additional $[Fe^{III}{}_3O]^{7+}$ triangle sharing a vertex at Fe2. Only one sao^{2-} ligand is present in the molecule, bridging in a $\eta^1{:}\eta^1{:}\eta^1{:}\mu$-mode between Fe5 and Fe6. The more prevalent ligand is the pdm^{2-} ligand, with six present in the molecule, all bridging in a $\eta^2{:}\eta^1{:}\eta^2{:}\mu_3$-mode, except for the one bridging Fe7-Fe8 which bridges only two metals in a $\eta^1{:}\eta^1{:}\eta^2{:}\mu$-mode. The four remaining edges are bridged by end-on N_3^- ligands, with three terminally bonded N_3^- ligands filling the remaining coordination sites on the Fe centres. The end-on bridging azide is particularly rare in Fe^{III} chemistry; a CCDC search revealing only two diiron complexes, each of which displays ferromagnetic exchange [54, 55]. Our previous efforts to incorporate azide bridges resulted in only a partial displacement (15%) of a μ-OMe^- bridge in the molecule $[Fe_8O_2(OMe)_{3.85}(N_3)_{4.15}(Me\text{-}sao)_6(py)_2]$ [16]. This makes **7** the first Fe^{III} cluster to contain end-on azide bridges of nuclearity greater than two. Eight of the Fe^{III} ions lie in distorted octahedral geometries with *cis* angles of 73.63(4)-128.39(4)° and *trans* angles of 138.45(4)-177.71(4)°. The remaining Fe ion (Fe4) is in a pentagonal bipyramidal geometry; equatorial angles between adjoining points on the pentagon are in the range 69.22(4)-79.16(4)°, angles between axial and equatorial sites are in the range 73.44(4)-105.20(4)° and the angle between the axial-axial sites is 176.79(4)°. All of the octahedral Fe^{III} centres have a $[O_4N_2]$ donor set and the pentagonal bipyramidal Fe^{III} centre has a $[O_5N_2]$ donor set. There are no inter-molecular hydrogen bonds, with the shortest contacts between neighbouring molecules being between a bridging azide ion and the pyridyl ring of a pdm^{2-} ligand (C…N 3.03(3) Å).

Magnetic Properties

Direct current (dc) magnetic susceptibility studies were performed for complexes **2**, **4**, **6** and **7** between 5-300 K in an applied field of 0.1 T. These are plotted as the $\chi_M T$ product versus T in Fig. (**6**). Complex **2** has a room temperature $\chi_M T$ value of 2.1 cm^3 K mol^{-1} which is considerably lower than the expected value for four non-interacting Fe^{III} centres (17.5 cm^3 K mol^{-1}) with g = 2.00, suggestive of strong antiferromagnetic exchange. The value of $\chi_M T$ continues to drop with decreasing temperature, reaching 0 cm^3 K mol^{-1} at ~25 K. The data can be fitted to the isotropic spin-Hamiltonian (1):

$$\hat{H} = -2J(\hat{S}_1 \cdot \hat{S}_2 + \hat{S}_1 \cdot \hat{S}_3 + \hat{S}_2 \cdot \hat{S}_4 + \hat{S}_3 \cdot \hat{S}_4) + \mu_B g B \sum_{i=1}^{4} \hat{S}_i \quad (1)$$

where J is the isotropic magnetic exchange interaction, $\hat{S}$ is a spin operator, μ_B is the Bohr magneton, g = 2 is the isotropic g-factor, B is the external magnetic field, the index i runs from 1 to 4 and we assume that all Fe^{III}…Fe^{III} interactions are equivalent. This affords J = -61 cm^{-1}. The S = 0 ground spin state is separated from the first excited (S = 1) state by 122 cm^{-1} (Fig. **7**). For comparison, the very similar complex $[L_2Fe_2(\mu_3\text{-}O)_2(salox)_2(diphenylglycolate)_3Fe_2](ClO_4)$ (L = 1,4,7-trimethyl-1,4,7-triazacyclononane) reported by Chaudhuri *et al* [25] has J = -41.4 cm^{-1} and all published J values of molecules with the Fe_4 butterfly topology fall in the range -33 to -46 cm^{-1} [56, 57]. Complexes **4** and **7** are described together as both display similar properties. Complexes **4** and **7** have room temperature $\chi_M T$ values of 12.43 cm^3 mol^{-1} K and 14.9 cm^3 mol^{-1} K, respectively, which are lower than the spin-only expected value (g = 2) for nine non-interacting Fe^{III} centres (39.375 cm^3 mol^{-1} K). This indicates the presence of dominant and relatively strong antiferromagnetic exchange between the metal centres. As the temperature is decreased the magnetic susceptibility decreases to values of 4.49 cm^3 mol^{-1} K for **4** and 4.1 cm^3 mol^{-1} K for **7** at 5 K. This suggests a small spin ground state (perhaps S = 5/2) for both, as one would expect for an odd-membered, antiferromagnetically coupled Fe^{III} cluster. The size of the metallic core and number of different exchange pathways preclude fitting of the susceptibility data. However, in order to shed further

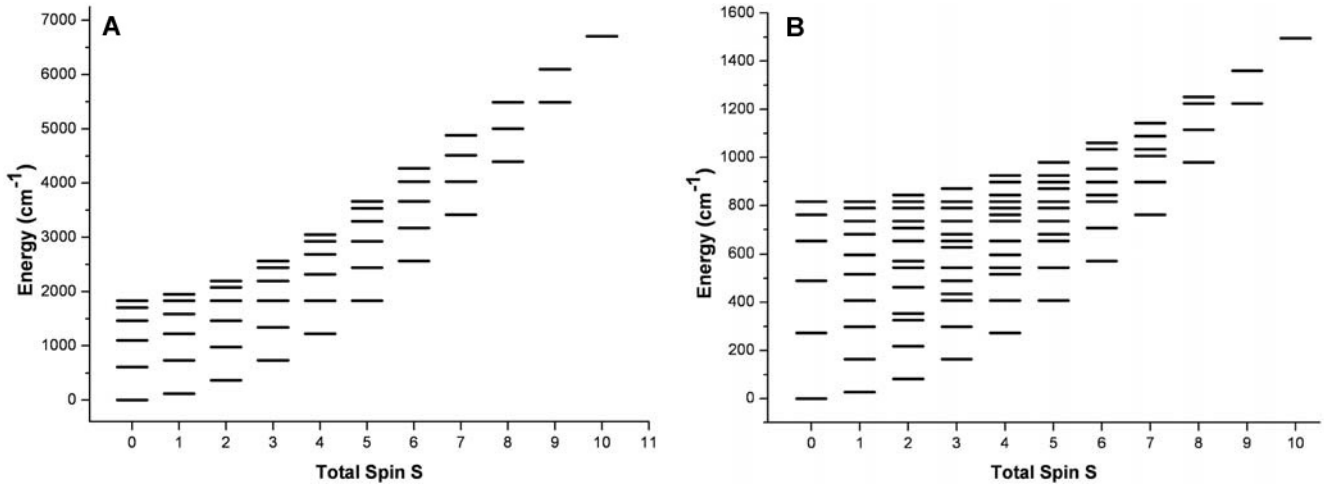

Fig. (7). Plot of energy versus total *S* state for complexes **2** (**A**) and **6** (**B**).

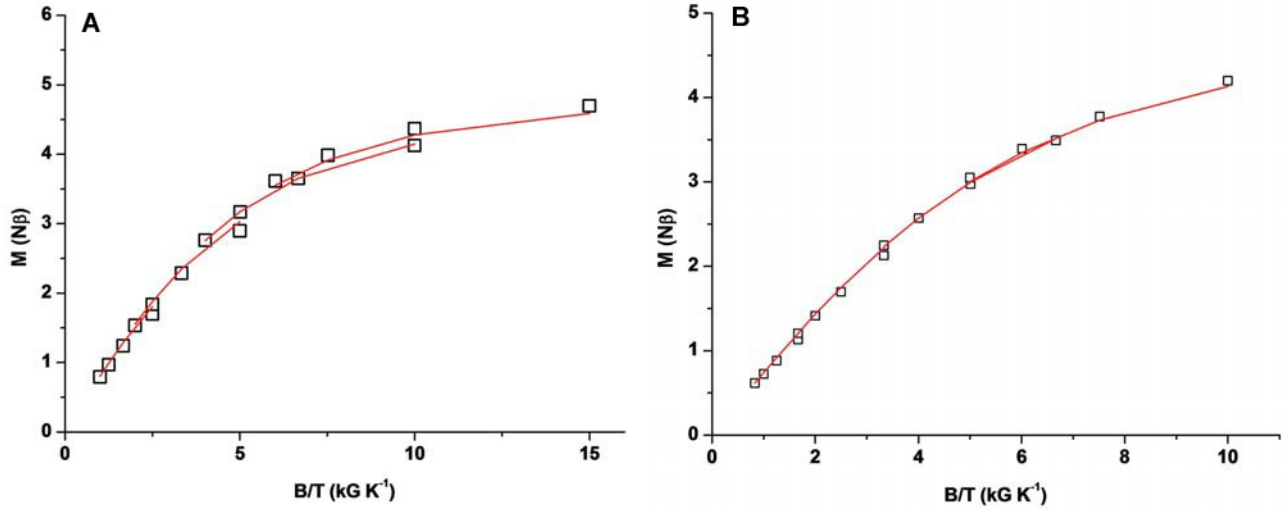

Fig. (8). Reduced magnetisation (M vs B/T) plots for complexes **4** (**A**) and **7** (**B**) in the 0.5, 1.0, 2.0 and 3.0 T and 2-5 K field and 2-5 K and 3-6 K temperature ranges, respectively. The solid red lines indicate the fit of the experimental data with the parameters given in the text.

light on the nature and identity of the ground state for complexes **4** and **7** field dependant magnetisation data (T = 2-7 K, B = 0.5-7.0 T) were collected (Fig. **8**), and the so-obtained data fitted to spin-Hamiltonian (2):

$$\hat{H} = D_S(\hat{S}_z^2 - S(S+1)/3) + \mu_B g B \hat{S} \quad (2)$$

where S is the total spin of the ground spin-state, D_S is the uniaxial anisotropy of the ground spin-state, g = 2, and we assume that only the ground spin-state is populated. This affords the following spin-Hamiltonian parameters: S = 5/2, $D_{(S=5/2)}$ = +0.653 cm^{-1} (**4**), and S = 5/2, $D_{(S=5/2)}$ = +0.301 cm^{-1} (**7**).

Complex **6** has a room temperature $\chi_M T$ value of 7.8 cm^3 mol^{-1} K, lower than the spin-only expected value (g = 2) for four non-interacting Fe^{III} centres (17.5 cm^3 K mol^{-1}). The $\chi_M T$ value decreases with decreasing temperature reaching 0 cm^3 K mol^{-1} by 10 K, indicative of comparatively strong antiferromagnetic interactions, resulting in a diamagnetic ground state. The data can again be fitted to the isotropic spin-Hamiltonian (1), in the same way as previously described. This affords an exchange interaction J = -13.6 cm^{-1} with the first excited (S = 1) state located 27.2 cm^{-1} above the S = 0 ground state (Fig. **7**). It is interesting to compare the exchange interactions for complexes **2** (mediated by oxime -N-O- and O^{2-}) and **6** (mediated by oxime -N-O- and $^{-}$OR), with the former almost five times stronger than the latter [58]. We can also compare the data for **6** to that previously reported for the complex $[Fe_4F_4(Ph\text{-}sao)_4(py)_4]$. The presence of more than one $[Fe_4]$ molecule in the unit cell of the latter complex precluded any fitting of the data, but a simple qualitative comparison of the data in Fig. (**6**) suggests that the exchange mediated by the F-bridges is somewhat weaker than that mediated by the alkoxides.

CONCLUSION

Seven new clusters have been added to the ever-growing family of polymetallic Fe^{III} clusters stabilised by salicylaldoxime-based ligands. The clusters have been synthesised by employing co-ligands (namely tacn, hmpH and $pdmH_2$) that are able to compete with the oxime ligands for the Fe coordination sites. This has resulted in a set of tetranuclear 'butterfly' clusters with the ligand tacn that display very strong antiferromagnetic exchange interactions and diamagnetic ground states. The pro-ligand hmpH produced three clusters:

two tetranuclear squares formed *via* two entirely different routes, and an unusual nonametallic cage. The related proligand $pdmH_2$ stabilised another intriguing [Fe_9] cluster containing some structural oddities. These include a rare example of Fe^{III} ions being bridged by end-on azides - previously observed in only two dinuclear clusters, and the first occurrence of a pentagonal bipyramidal Fe^{III} centre in Fe-salicylaldoxime chemistry.

CONFLICT OF INTEREST

The authors confirm that this article content has no conflicts of interest.

ACKNOWLEDGEMENTS

EKB thanks the Leverhulme Trust and EPSRC for funding.

REFERENCES

[1] Khanra, S.; Helliwell, M.; Tuna, F.; McInnes, E. J. L.; Winpenny, R. E. P. Synthesis, structural characterisation and magnetic studies of polymetallic iron phosphonate cages. *Dalton Trans.,* **2009,** (31), 6166-6174.

[2] Miao, Y.L.; Liu, J.L.; Lin, Z.J.; Ou, Y.C.; Leng, J.D.; Tong, M.L. Synthesis, structures, adsorption behaviour and magnetic properties of a new family of polynuclear iron clusters. *Dalton Trans.,* **2010,** *39*(20), 4893-4902.

[3] Malone, S.A.; Lewin, A.; Kilic, M.A.; Svistunenko, D.A.; Cooper, C.E.; Wilson, M.T.; Le Brun, N.E.; Spiro, S.; Moore, G.R. Protein-Template-Driven Formation of Polynuclear Iron Species. *J. Am. Chem. Soc.,* **2004,** *126*, 496-504.

[4] Theil, E.C. Ferritin: Structure, Gene regulation, and cellular function in animals, plants, and microorganisms. *Annu. Rev. Biochem.,* **1986,** *56*, 289-315.

[5] Xu, B.; Chasteen, N.D. Iron Oxidation Chemistry in Ferritin. *J. Biol. Chem.,* **1991,** *266*, 19965-19970.

[6] Greedan, J.E. Geometrically frustrated magnetic materials. *J. Mater. Chem.,* **2001,** *11*(1), 37-53.

[7] Fardis, M.; Diamantopoulos, G.; Karayianni, M.; Papavassiliou, G.; Tangoulis, V.; Konsta, A. ^{1}H NMR investigation of the spin dynamics of the spin-frustrated trinuclear Fe cluster $(NH_4)[Fe_3(\mu_3\text{-}OH)(H_2L)_3(HL)_3](H_3L$=orotic acid). *Phys. Rev. B.,* **2001,** *65*(1), 014412.

[8] van Slageren, J.; Rosa, P.; Caneschi, A.; Sessoli, R.; Casellas, H.; Rakitin, Y.V.; Cianchi, L.; Giallo, F.D.; Spina, G.; Bino, A.; Barra, A.L.; Guidi, T.; Carretta, S.; Caciuffo, R. Static and dynamic magnetic properties of an [Fe_{13}] cluster. *Phys. Rev. B.,* **2006,** *73*(1), 014422.

[9] Garlea, V.O.; Nagler, S.E.; Zarestky, J.L.; Stassis, C.; Vaknin, D.; Kögerler, P.; McMorrow, D.F.; Niedermayer, C.; Tennant, D.A.; Lake, B.; Qiu, Y.; Exler, M.; Schnack, J.; Luban, M. Probing spin frustration in high-symmetry magnetic nanomolecules by inelastic neutron scattering. *Phys. Rev. B.,* **2006,** *73*(2), 024414.

[10] Schnack, J.; Luban, M.; Modler, R. Quantum rotational band model for the Heisenberg molecular magnet {Mo_{72} Fe_{30}}. *Europhys. Lett.,* **2001,** *56*(6), 863-869.

[11] Evangelisti, M.; Brechin, E.K. Recipes for enhanced molecular cooling. *Dalton Trans.,* **2010,** *39*(20), 4672-4676.

[12] Evangelisti, M.; Candini, A.; Ghirri, A.; Affronte, M.; Brechin, E.K.; McInnes, E.J.L. Spin-enhanced magnetocaloric effect in molecular nanomagnets. *Appl. Phys. Lett.,* **2005,** *87*(7), 072504.

[13] Gass, I.A.; Milios, C.J.; Collins, A.; White, F.J.; Budd, L.; Parsons, S.; Murrie, M.; Perlepes, S.P.; Brechin, E.K. Polymetallic clusters of iron(iii) with derivatised salicylaldoximes. *Dalton Trans.,* **2008,** *15*, 2043-2053.

[14] Mason, K.; Chang, J.; Garlatti, E.; Prescimone, A.; Yoshii, S.; Nojiri, H.; Schnack, J.; Tasker, P. A.; Carretta, S.; Brechin, E.K. Linking [FeIII3] triangles with "double-headed"phenolic oximes. *Chem. Commun.,* **2011,** *47*(21), 6018-6020.

[15] Mason, K.; Gass, I.A.; Parsons, S.; Collins, A.; White, F.J.; Slawin, A.M.Z.; Brechin, E.K.; Tasker, P.A. Building Fe(iii) clusters with derivatised salicylaldoximes. *Dalton Trans.,* **2010,** *39*(10), 2727-2734.

[16] Mason, K.; Gass, I.A.; White, F.J.; Papaefstathiou, G.S.; Brechin, E.K.; Tasker, P.A. Hexa- and octanuclear iron(iii) salicylaldoxime clusters. *Dalton Trans.,* **2011,** *40*(12), 2875-2881.

[17] Gass, I.A.; Milios, C.J.; Whittaker, A.G.; Fabiani, F.P.A.; Parsons, S.; Murrie, M.; Perlepes, S.P.; Brechin, E.K. A Cube in a Tetrahedron: Microwave-Assisted Synthesis of an Octametallic FeIII Cluster. *Inorg. Chem.,* **2006,** *45*(14), 5281-5283.

[18] Babu, M.S.S.; Reddy, K.H.; Krishna, P.G. Synthesis, characterization, DNA interaction and cleavage activity of new mixed ligand copper(II) complexes with heterocyclic bases. *Polyhedron,* **2007,** *26*(3), 572-580.

[19] Tasker, P.A.; Plieger, P.G.; West, L.C. Metal complexes for Hydrometallurgy and Extraction. *Comprehensive Coordination Chemistry II,* **2004,** *9*, 759.

[20] Tasker, P.A.; Tong, C.C.; Westra, A.N. Co-extraction of cations and anions in base metal recovery. *Coord. Chem. Rev.,* **2007,** *251*(13-14), 1868-1877.

[21] Kordosky, G.A. *Proc. Int. Solvent Extr. Conf.,* **2002**, 853-862.

[22] Mackey, P.J.; *CIM Mag.,* **2007,** *2*, 35-42.

[23] Thorpe, J.M.; Beddoes, R.L.; Collison, D.; Garner, C.D.; Helliwell, M.; Holmes, J.M.; Tasker, P.A. Surface Coordination Chemistry: Corrosion Inhibition by Tetranuclear Cluster Formation of Iron with Salicylaldoxime. *Angew. Chem. Int. Ed.,* **1999,** *38*(8), 1119-1121.

[24] Bill, E.; Krebs, C.; Winter, M.; Gerdan, M.; Trautwein, A.X.; Flörke, U.; Haupt, H.J.; Chaudhuri, P. A Triangular Iron(III) Complex Potentially Relevant to Iron(III)-Binding Sites in Ferreascidin. *Chem. Eur. J.,* **1997,** *3*(2), 193-201.

[25] Chaudhuri, P.; Rentschler, E.; Birkelbach, F.; Krebs, C.; Bill, E.; Weyhermüller, T.; Flörke, U. Ground Spin State Variation in Carboxylate-Bridged Tetranuclear [Fe2Mn2O2]$^{8+}$ Cores and a Comparison with Their [Fe_4O_2]$^{8+}$ and [Mn_4O_2]$^{8+}$ Congeners. *Eur. J. Inorg. Chem.,* **2003,** *2003*(3), 541-555.

[26] Chaudhuri, P.; Winter, M.; Fleischhauer, P.; Haase, W.; Flörke, U.; Haupt, H.J.r. Synthesis, structure and magnetism of a tetranuclear Fe(III) complex containing an [$Fe_4(\mu_3\text{-}O)_2$]$^{8+}$ core. *Inorg. Chem. Acta.,* **1993,** *212*(1-2), 241-249.

[27] Raptopoulou, C.P.; Boudalis, A.K.; Sanakis, Y.; Psycharis, V.; Clemente-Juan, J.M.; Fardis, M.; Diamantopoulos, G.; Papavassiliou, G. Hexanuclear Iron(III) Salicylaldoximato Complexes Presenting the [$Fe_6(\mu_3\text{-}O)_2(\mu_2\text{-}OR)_2$]$^{12+}$ Core: Syntheses, Crystal Structures, and Spectroscopic and Magnetic Characterization. *Inorg. Chem.,* **2006,** *45*(5), 2317-2326.

[28] Raptopoulou, C.P.; Sanakis, Y.; Boudalis, A.K.; Psycharis, V. Salicylaldoxime (H2salox) in iron(III) carboxylate chemistry: Synthesis, X-ray crystal structure, spectroscopic characterization and magnetic behavior of trinuclear oxo-centered complexes. *Polyhedron,* **2005,** *24*(5), 711-721.

[29] Verani, C.N.; Bothe, E.; Burdinski, D.; Weyhermüller, T.; Flörke, U.; Chaudhuri, P. Synthesis, Structure, Electrochemistry, and Magnetism of [$Mn^{III}Mn^{III}$], [$Mn^{III}Fe^{III}$] and [$Fe^{III}Fe^{III}$] Cores: Generation of Phenoxyl Radical Containing [$Fe^{III}Fe^{III}$] Species. *Eur. J. Inorg. Chem.,* **2001,** *2001*(8), 2161-2169.

[30] Brechin, E.K.; Knapp, M.J.; Huffman, J.C.; Hendrickson, D.N.; Christou, G. New hexanuclear and octanuclear iron(III) oxide clusters: octahedral [Fe_6O_2]$^{14+}$ species and core isomerism in [Fe_8O_4]$^{16+}$ complexes. *Inorg. Chim. Acta.,* **2000,** *297*(1-2), 389-399.

[31] Christmas, C.A.; Tsai, H.L.; Pardi, L.; Kesselman, J.M.; Gantzel, P.K.; Chadha, R.K.; Gatteschi, D.; Harvey, D.F.; Hendrickson, D.N. Hexanuclear ferric complexes possessing different degrees of spin frustration. *J. Am. Chem. Soc.,* **1993,** *115*(26), 12483-12490.

[32] Clemente-Juan, J.M.; Mackiewicz, C.; Verelst, M.; Dahan, F.; Bousseksou, A.; Sanakis, Y.; Tuchagues, J.P. Synthesis, Structure, and Magnetic Properties of Tetranuclear Cubane-like and Chain-like Iron(II) Complexes Based on the N4O Pentadentate Dinucleating Ligand 1,5-Bis[(2-pyridylmethyl)amino]pentan-3-ol. *Inorg. Chem.,* **2002,** *41*(6), 1478-1491.

[33] Drüeke, S.; Wieghardt, K.; Nuber, B.; Weiss, J.; Bominaar, E.L.; Sawaryn, A.; Winkler, H.; Trautwein, A. X. A new tetranuclear oxohydroxoiron(III) cluster: crystal structure, magnetic properties, and EXAFS investigation of [$L_4Fe_4(\mu\text{-}O)_2(\mu\text{-}OH)_4$]$I_4 \cdot 3H_2O$ (L = 1,4,7-triazacyclononane). *Inorg. Chem.,* **1989,** *28*(25), 4477-4483.

[34] Poganiuch, P.; Liu, S.; Papaefthymiou, G.C.; Lippard, S.J. Trinuclear, oxo-centered mixed-valence iron complex with unprecedented carboxylate coordination: $[Fe_3O(O_2CCH_3)_6(TACN)]\cdot 2CHCl_3$. *J. Am. Chem. Soc.,* **1991,** *113*(12), 4645-4651.

[35] Taguchi, T.; Stamatatos, T.C.; Abboud, K.A.; Jones, C.M.; Poole, K.M.; O'Brien, T.A.; Christou, G. New Fe4, Fe6, and Fe8 Clusters of Iron(III) from the Use of 2-Pyridyl Alcohols: Structural, Magnetic, and Computational Characterization. *Inorg. Chem.,* **2008,** *47*(10), 4095-4108.

[36] Taguchi, T.; Thompson, M.S.; Abboud, K.A.; Christou, G. Unusual Fe_9 and Fe_{18} structural types from the use of 2,6-pyridinedimethanol in FeIII cluster chemistry. *Dalton Trans.,* **2010,** *39*(38), 9131-9139.

[37]) Wieghardt, K.; Bossek, U.; Gebert, W. Synthesis of a Tetranuclear Manganese(IV) Cluster with Adamantane Skeleton: $[(C_6H_{15}N_3)_4Mn4O_6]^{4+}$. *Angew. Chem. Int. Ed.,* **1983,** *22*(4), 328-329.

[38] Wieghardt, K.; Pohl, K.; Gebert, W. $[\{(C_6H_{15}N_3)Fe\}_2(\mu\text{-}O)(\mu\text{-}CH_3CO_2)_2]^{2+}$ a Dinuclear Iron (III)Complex with a Metazidohemerythrin-Type Structure. *Angew. Chem. Int. Ed.,* **1983,** *22*(9), 727-727.

[39] Weighardt, K.; Pohl, K.; Jibril, I.; Huttner, G. Hydrolysis Products of the Monomeric Amine Complex (C6H15N3)FeCl3: The Structure of the Octameric Iron(III) Cation of $\{[(C_6H_{15}N_3)_6Fe_8(\mu_3\text{-}O)_2(\mu_2\text{-}OH)_{12}]Br_7(H_2O)\}Br\cdot 8H_2O$. *Angew. Chem. Int. Ed.,* **1984,** *23*(1), 77-78.

[40] Barra, A.L.; Caneschi, A.; Cornia, A.; Fabrizi de Biani, F.; Gatteschi, D.; Sangregorio, C.; Sessoli, R.; Sorace, L. Single-Molecule Magnet Behavior of a Tetranuclear Iron(III) Complex. The Origin of Slow Magnetic Relaxation in Iron(III) Clusters. *J. Am. Chem. Soc.,* **1999,** *121*(22), 5302-5310.

[41] Barra, A.L.; Bencini, F.; Caneschi, A.; Gatteschi, D.; Paulsen, C.; Sangregorio, C.; Sessoli, R.; Sorace, L. Tuning the Magnetic Properties of the High-Spin Molecular Cluster Fe_8. *Chem. Phys. Chem.,* **2001,** *2*(8-9), 523-531.

[42] Boskovic, C.; Brechin, E.K.; Streib, W.E.; Folting, K.; Bollinger, J.C.; Hendrickson, D.N.; Christou, G. Single-Molecule Magnets: A New Family of Mn_{12} Clusters of Formula $[Mn_{12}O_8X_4(O_2CPh)_8L_6]$. *J. Am. Chem. Soc.,* **2002,** *124*(14), 3725-3736.

[43] Boskovic, C.; Wernsdorfer, W.; Folting, K.; Huffman, J.C.; Hendrickson, D.N.; Christou, G. Single-Molecule Magnets: Novel Mn_8 and Mn_9 Carboxylate Clusters Containing an Unusual Pentadentate Ligand Derived from Pyridine-2,6-dimethanol. *Inorg. Chem.,* **2002,** *41*(20), 5107-5118.

[44] Harden, N.C.; Bolcar, M.A.; Wernsdorfer, W.; Abboud, K.A.; Streib, W.E.; Christou, G. Heptanuclear and Decanuclear Manganese Complexes with the Anion of 2-Hydroxymethylpyridine. *Inorg. Chem.,* **2003,** *42*(22), 7067-7076.

[45] Lecren, L.; Roubeau, O.; Coulon, C.; Li, Y.G.; Le Goff, X.F.; Wernsdorfer, W.; Miyasaka, H.; Clérac, R. Slow Relaxation in a One-Dimensional Rational Assembly of Antiferromagnetically Coupled $[Mn_4]$ Single-Molecule Magnets. *J. Am. Chem. Soc.,* **2005,** *127*(49), 17353-17363.

[46] Murugesu, M.; Habrych, M.; Wernsdorfer, W.; Abboud, K.A.; Christou, G. Single-Molecule Magnets: A Mn_{25} Complex with a Record S = 51/2 Spin for a Molecular Species. *J. Am. Chem. Soc.,* **2004,** *126*(15), 4766-4767.

[47] Sañudo, E.C.; Brechin, E.K.; Boskovic, C.; Wernsdorfer, W.; Yoo, J.; Yamaguchi, A.; Concolino, T.R.; Abboud, K.A.; Rheingold, A.L.; Ishimoto, H.; Hendrickson, D.N.; Christou, G. $[Mn_{18}]^{2+}$ and $[Mn_{21}]^{4+}$ single-molecule magnets. *Polyhedron,* **2003,** *22*(14-17), 2267-2271.

[48] Stamatatos, T.C.; Abboud, K.A.; Wernsdorfer, W.; Christou, G. High-Nuclearity, High-Symmetry, High-Spin Molecules: A Mixed-Valence Mn_{10} Cage Possessing Rare T symmetry and an S=22 Ground State. *Angew. Chem. Int. Ed.,* **2006,** *45*(25), 4134-4137.

[49] Stamatatos, T.C.; Poole, K.M.; Abboud, K.A.; Wernsdorfer, W.; O'Brien, T.A.; Christou, G. High-Spin Mn_4 and Mn_{10} Molecules: Large Spin Changes with Structure in Mixed-Valence MnII4MnIII6 Clusters with Azide and Alkoxide-Based Ligands. *Inorg. Chem.,* **2008,** *47*(11), 5006-5021.

[50] Stamatatos, T.C.; Vlahopoulou, G.C.; Raptopoulou, C.P.; Terzis, A.; Escuer, A.; Perlepes, S.P. Interpretation of the Magnetic Properties of a Compound Consisting of Cocrystallized Cu^{II}_3 and Cu^{II}_4 Clusters through the Targeted Synthesis and Study of Its Discrete CuII4 Component. *Inorg. Chem.,* **2009,** *48*(11), 4610-4612.

[51] Yang, E.C.; Wernsdorfer, W.; Zakharov, L.N.; Karaki, Y.; Yamaguchi, A.; Isidro, R.M.; Lu, G.D.; Wilson, S.A.; Rheingold, A.L.; Ishimoto, H.; Hendrickson, D.N. Fast Magnetization Tunneling in Tetranickel(II) Single-Molecule Magnets. *Inorg. Chem.,* **2005,** *45*(2), 529-546.

[52] Dunstan, W.R.; Henry, T.A., VIII. Occurrence of orthohydroxyacetophenone in the volatile oil of Chione glabra. *J. Chem. Soc., Trans.,* **1899,** *75*, 66-71.

[53] Wieghardt, K.; Schmidt, W.; Nuber, B.; Weiss, J. Neue μ-Hydroxo-Übergangsmetallkomplexe, I. Darstellung und Struktur des trans-Diaqua-di-μ-hydroxo-bis[(1,4,7-triazacyclononan)cobalt(III)]-Kations; Kinetik und Mechanismus seiner Bildung. *Chem. Ber.,* **1979,** *112*(6), 2220-2230.

[54] De Munno, G.; Poerio, T.; Viau, G.; Julve, M.; Lloret, F. Ferromagnetic Coupling in the Bis(μ-end-on-azido)iron(III) Dinuclear Complex Anion of $[Fe^{II}(bpym)_3]_2[Fe^{III}_2(N_3)_{10}]\cdot 2H_2O$. *Angew. Chem. Int. Ed.,* **1997,** *36*(13-14), 1459-1461.

[55] Reddy, K.R.; Rajasekharan, M.V.; Tuchagues, J.P. Synthesis, Structure, and Magnetic Properties of Mn(salpn)N3, a Helical Polymer, and Fe(salpn)N3, a Ferromagnetically Coupled Dimer (salpnH2 = N,N′-bis(Salicylidene)-1,3-diaminopropane). *Inorg. Chem.,* **1998,** *37*(23), 5978-5982.

[56] Cauchy, T.; Ruiz, E.; Alvarez, S. Magnetostructural Correlations in Polynuclear Complexes: The Fe_4 Butterflies. *J. Am. Chem. Soc.;* **2006,** *128*(49), 15722-15727.

[57] Gomez-Coca, S.; Cauchy, T.; Ruiz, E. Extended Fe_4 butterfly complexes: theoretical analysis of magnetic properties and magnetostructural maps. *Dalton Trans.,* **2010,** *39*(20), 4832-4837.

[58] Weihe, H.; Güdel, H.U. Angular and Distance Dependence of the Magnetic Properties of Oxo-Bridged Iron(III) Dimers. *J. Am. Chem. Soc.,* **1997,** *119*(28), 6539-6543.

Received: March 07, 2013 Revised: April 09, 2013 Accepted: April 09, 2013